

Development of Nonhydrostatic Coupled Ocean–Atmosphere Simulation Code

Group Representative

Keiko Takahashi The Earth Simulator Center

Author

Keiko Takahashi The Earth Simulator Center

Nonhydrostatic coupled ocean-atmosphere simulation code has been developed in the Earth Simulator Center since the beginning of FY2003. For the first step to validate of our simulation code, various experiments were performed and a part of result is presented in this report. Nonhydrostatic global atmosphere component with 2.6 km resolution for horizontal and 96 vertical layers has achieved 60% to the theoretical peak performance using 512 nodes of the Earth Simulator.

Keywords: Nonhydrostatic, Coupled ocean-atmosphere global circulation model, High performance computation, The Earth Simulator

1. Introduction

The Earth Simulator have brought us a mean state of global simulation with ultra high horizontal resolution. Furthermore, for regional meteorological simulation, several weeks' weather prediction with a few kilometer horizontal resolution has been promoted in authorized Earth Simulator Projects. Toward the next step, when climate change has happened, it will be required that we can argue clearly about what local climate and local weather become. The answer to these questions is just information we want to know. Even though there is difficulties to argue about interactions between local and global weather/climate phenomena, many efforts will have to be made for the grand challenge.

In the Earth Simulator Center, we have just started developing nonhydrostatic coupled ocean-atmosphere simulation code on the sphere with high computational performance, which can represent mesoscale processes of such as typhoon, concentrated downpour, cumulus, tornado, downburst. This approach should bring us useful research tools to consider global climate and the local weather/climate simultaneously.

In this report, at the first step of development, we show preliminary results from simulations using atmosphere or ocean components. Each of components codes is designed and built from the scratch in the Earth Simulator Center. Grid system, discretization and interpolation schemes are described in section 2. Results from benchmark test experiments and computational performance on the Earth Simulator are presented in section 3–4.

2. Design of components

2.1. Grid system and governing equations

Introduced Yin-Yang grid system has been proposed by Solid Earth Simulation Group of the Earth Simulator Center (Figure 1). This system is composed of two latitude/longitude grid panels, which are called N- and E-systems. In the grid system, the south and north poles are not treated as singular points. In addition, Courant-Friedrichs-Lewy condition is relaxed comparing it in latitude/longitude grid system.

In nonhydrostatic atmospheric component of the coupled model, fully compressive three-dimensional Navier-Stokes equations with rotational effects (i), continuity equation (ii), pressure equation (iii) and equation of the state (iv) are used as follows. Perturbation density, three components of momentum and perturbation pressure are set as forecast variables. Discretization and integration schemes are shown in Table 1.

$$\frac{\partial \rho \mathbf{v}}{\partial t} + \nabla p' + \rho' \mathbf{g} = -\nabla \cdot (\rho \mathbf{v} \mathbf{v}) + 2\rho \mathbf{v} \times \mathbf{f} + \mu \left(\nabla^2 \mathbf{v} + \frac{1}{3} \nabla \cdot (\nabla \mathbf{v}) \right) \quad (\text{i})$$

$$\frac{\partial \rho'}{\partial t} + \nabla \cdot (\rho \mathbf{v}) = 0 \quad (\text{ii})$$

$$\frac{\partial P'}{\partial t} + \bar{\rho} \mathbf{g} \cdot \mathbf{w} + \mathbf{v} \cdot \nabla P' + \gamma P' \nabla \cdot \mathbf{v} = (\gamma - 1) \kappa \nabla^2 T + (\gamma - 1) \Phi \quad (\text{iii})$$

$$P = \rho RT \quad (\text{iv})$$

For advanced high resolution simulation of ocean dynamics, tide scheme and momentum/thermodynamic equations for compressible Boussinesq fluid are introduced. Discretization for time and space is specified as well as schemes in the



Fig. 1 Yin-Yang grid system.

Table 1 Simulation code specification.

Coordinate/staggering	horizontal	Yin-Yang grid with 3D-Coriolis, Arakawa-C
	vertical	Z* coordinate/ Lorenz staggering
Space- and time-schemes	HE-VI method, 3 rd order Runge-Kutta with Forward-Backward	
Advection scheme	CIP-CSLR	
Conservation	Mass	
Boundary on upper and bottom	Vertical velocity without motion and free slip	
Diffusion/viscosity	2 nd order diffusion and viscosity	
Damping/filtering	Divergence damping for 3d-wind, Rayleigh damping for momentum	

atmospheric component. Furthermore, Poisson solver for huge problems, which was developed originally in the Earth Simulator Center, is adopted in ocean code.

Taking account of interactions between atmosphere and ocean with ultra high resolution, which play important roles in representing of structure of mixed layer in the ocean, advanced techniques for estimation of fluxes have been introduced.

3. Numerical simulation and validation

3.1. Mass conserving numerical scheme

One of essential issues on overset grid systems such as Yin-Yang grid is mass conservation problem. We have introduced a mass imbalance correction scheme in interpolated velocity field.

Schematic image for the conservative scheme on a boundary is shown in Figure 2. For flux F_{EF} on a circular arc EF shown as red circle in Figure 2, sufficient condition for mass conservation holds as following (V). The condition means that the budget of fluxes f_N by calculated f_1, f_2, f_3 and f_4 on a grid ABCD of N system is equal to flux f_E estimated by fluxes f_{11} and f_{21} on a circular arc GHI of E system.

$$F_{EF} = \int_{\Gamma_{EF}} f_E d\Gamma = \int_{\Gamma_{EF}} f_N d\Gamma \quad (v)$$

Using this conservative scheme, we have evaluated that that time evolution of relative error of the mass has changed within the limit of rounding error.

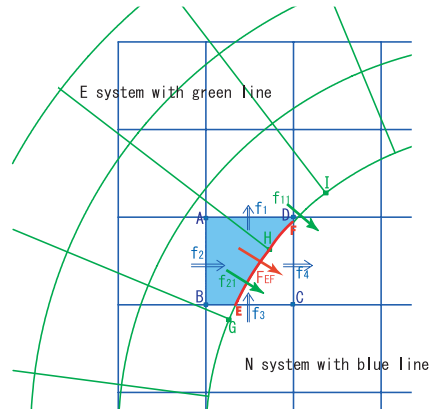


Fig. 2 Conserving interpolation scheme on boundary.

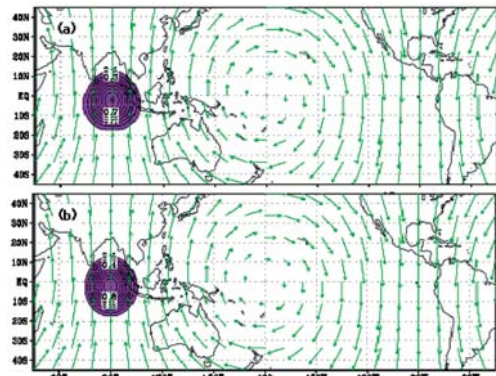


Fig. 3 Advection test with Courant number = 3. Result with 250 km horizontal resolution is shown in (a), and with 60 km horizontal resolution is shown as (b), respectively.

3.2. Conservative semi-Lagrangian transport scheme based on CIP

Conservative semi-Lagrangian scheme with rational function (CIP-CSLR) based on Cubic-interpolated pseudo-particle (CIP) has introduced to the atmospheric component. High-accuracy of CIP-CSLR has already been shown in previous studies. Figure 3 presents that large Courant number is available without numerical error in Williamson test case 1 for the shallow water equation. Those results show CIP-CSLR scheme should be used for large Courant number without remarkable errors.

3.3. Numerical sensitivity experiments to shallow water equations

Williamson test cases 2 and 6 experiments with 60km horizontal resolution are presented. Test case 2 is to validate a steady state solution to the non-linear zonal geostrophic flow. Test case 6 initialized by Rossby-Haurwitz waves is to validate possibility of growth of unstable mode. Results of test 2 and 6 shows sufficient performance compared with ordinary results (Figure 4 and 5) although test 6 is required to continue longer integration.

3.4. Vertical differencing of primitive equations

In order to extend three dimensional simulation, characteristic of vertical staggering is one of basic problems. 24 cases, which are whole combinatorial cases of Lorenz types and Charney-Phillips types vertical staggering, were examined to identify those features. Charney-Phillips type distribution, case B2 in Figure 6, shows best features to propagation vertical waves, though it is required to dissipate 2 grid oscillations due to the vertical distribution.

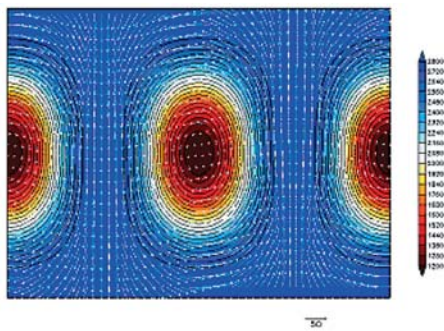


Fig. 4 Results of test case 2 after 5 day's integration.

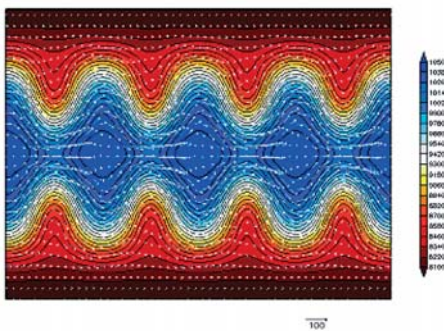


Fig. 5 Results of test case 6 after 1 day's integration.

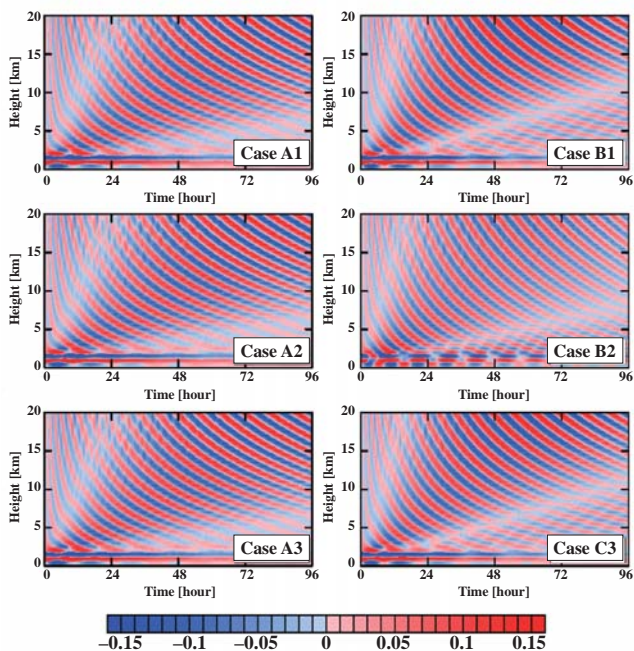


Fig. 6 Characteristics of wave propagation due to vertical differencing.

3.5. 3-dimensional simulation of nonhydrostatic mountain waves and Held and Suarez experiments

In order to verify the accuracy of the metric term, 3-dimensional mountain wave experiments were performed. The height of the top is 40 km and 24 vertical layers are settled. An isolated bell-shaped mountain with 1000 m height located on (0N, 180N) was employed and uniform zonal mean easterly flow 40 m /sec was specified. These results showed that integrations was possible without influence of the overlapped portion as shown in Figure 7.

To evaluate the long-term statistical properties of a fully developed general circulation, a benchmark calculation proposed by Held and Suarez was carried out. Figure 8 shows zonal mean wind distribution after 1000 days integration. Results were comparable with previous studies.

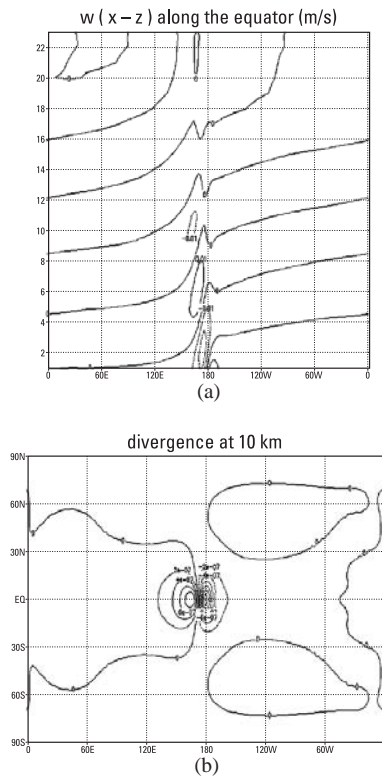


Fig. 7 Snapshot of experiments with a mountain located on (0N, 180E). (a): cross section of vertical wind speed, (b) is horizontal divergence, respectively, after 30 days integration.

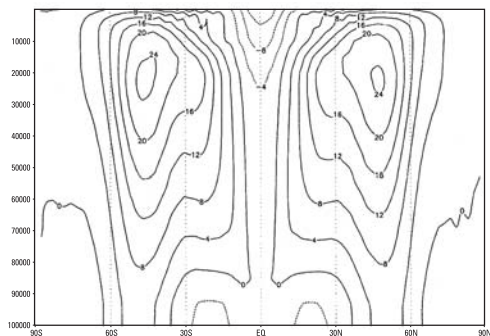


Fig. 8 Zonal mean wind of Held and Suarez experiments.

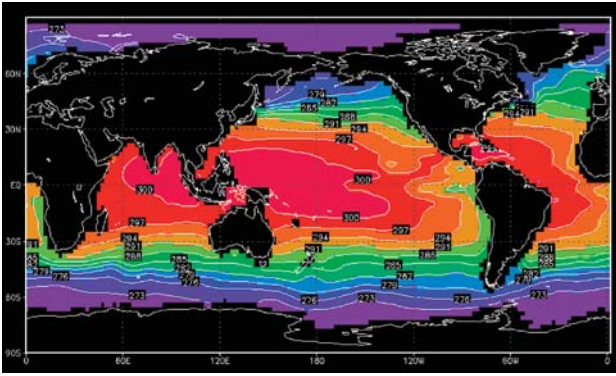


Fig. 9 Sea surface temperature distribution after several months' integration.

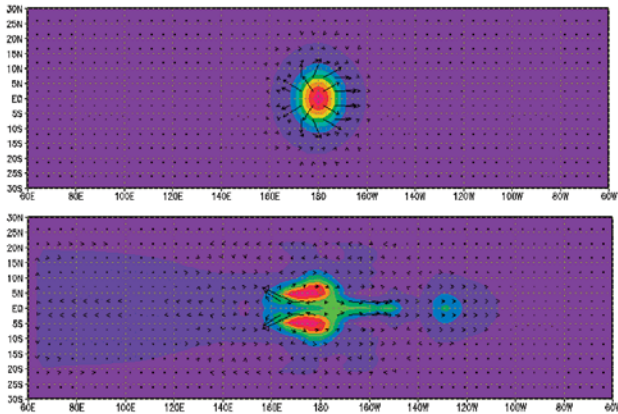


Fig.10 Propagation of Kelvin waves in equatorial region.

3.6. 3-dimensional nonhydrostatic ocean general circulation simulation

A mean state obtained by preliminary simulation using introduced non-hydrostatic ocean global circulation is presented in Figure 9. Resolution was 100 km for horizontal and 50 layers for vertical. Initial state and boundaries were given as climatologically monthly data. Although of course nonhydrostatic characteristics does not appear with this resolution and land-sea distribution was specified without bottom topography in this simulation, SST mean state is comparable to previous studies. As additional validations of basic performances, equatorial waves characterized by Kelvin/Rossby waves and internal gravity waves (not shown) were validated (Figure 10). The results were also comparable with conventional theoretical features.

3.7. Mean state of 3-dimensional atmospheric global circulation with real orography

In Figure 11, wind distribution in the Himalaya region are presented after 48 hours integration by non-hydrostatic atmospheric global circulation code with 80 km resolution for horizontal and 96 vertical layers. Fine structure was reproduced and the nonhydrostatic code on the sphere was performed without no problem under conditions that hydrostatic equilibrium was satisfied.

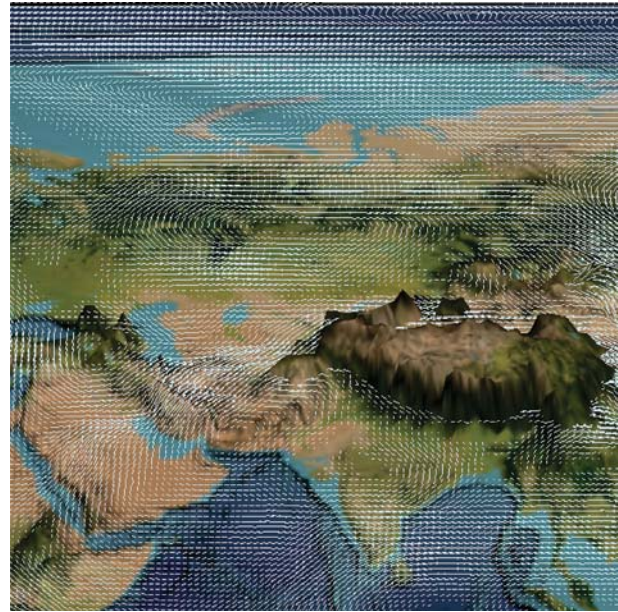
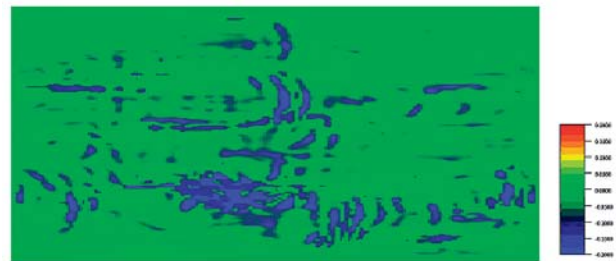


Fig.11 Wind vector distribution near Himalaya region at 750 hPa.



(a) Reynolds stress distributions.



(b) Instantaneous interface distributions.

Fig.12 Evaluation of surface interaction using C-CUP method.

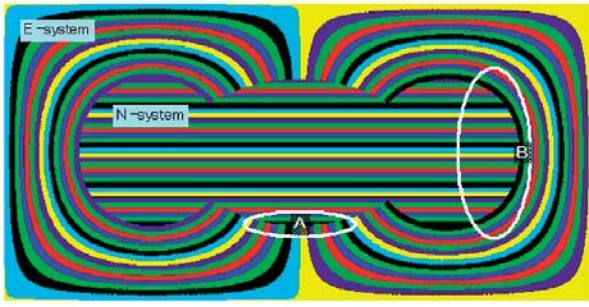
3.8. Interaction between atmosphere and ocean

Advanced approach to deal with interface between atmosphere and ocean should be thought as gas-liquid interaction at turbulent free surface. C-CUP (CIP-combined unified procedure) method was proposed in order to estimate momentum transport near surface. Figure 12 shows instantaneous Reynolds stress distributions and instantaneous interface distributions near the interface were in well correlation in their structures. This suggests that the momentum transportation significantly depend on the fluctuation of the interface.

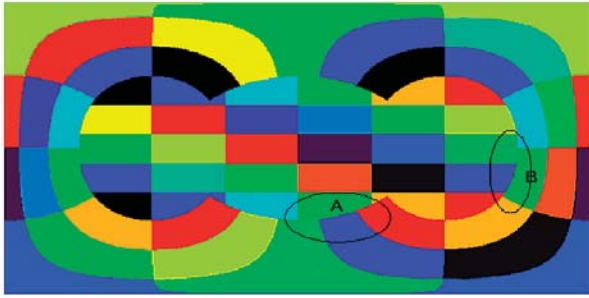
4. Optimized parallel computation on the Earth Simulator

4.1. Strategic parallelization and performance

Perimeter of each colored region in schematic Figure 13 is corresponding to a mount of communication between processes. The number of neighborhood of each region is



(a) Communication with 1-dimensional decomposition.



(b) Communication for two-dimensional distribution.

Fig.13 Communication cost imbalance on boundary regions under the same number of nodes.

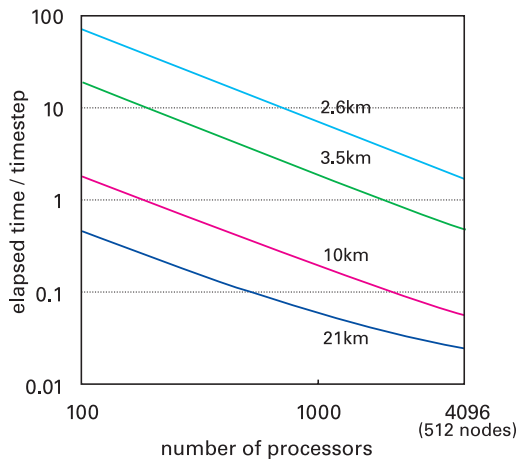


Fig.14 Performance statistics on the Earth Simulator.

equal to the number of nodes to be communicated. Because communication cost can be reduced with 2-dimensional decomposition and computational cost imbalance between A and B regions can be avoided, 2-dimensional decomposition was adopted. For inter-node parallel processing, MPI library was used. Microtasking architecture was used for intra-node parallel processing.

Figure 14 shows computational performance statistics of our code with different horizontal resolution on the Earth Simulator. The performance was estimated for dynamical core of the introduced atmospheric simulation code.

Table 2 Current status of performance.

[km]	resolution grid points	#of nodes	peak ratio [%]	V.Op.Ratio [%]	VLEN
20.9	$1440 \times 480 \times 96 \times 2$	6	58.1	99.53	236.8
10.4	$2880 \times 960 \times 96 \times 2$	24	56.7	99.52	237.4
5.2	$5760 \times 1920 \times 96 \times 2$	96	59.9	99.54	239.2
3.5	$8640 \times 2880 \times 96 \times 2$	216	60.0	99.54	238.9
2.6	$11520 \times 3840 \times 96 \times 2$	512	59.9	99.60	239.7

Comparing the statistics between of AFES and our code with 10 km resolution for horizontal, our code is 10 times faster as CPU time even without CIP semi-Lagrangian scheme. Computational performance with 2.6 km horizontal resolution has attained to about 60% of the theoretical peak performance 32.8 Tflops of 4096 processors (512 nodes). Current status of computational performance is shown in Table 2.

4.2. Poisson equations with implicit schemes

2-dimensional Poisson solvers with high parallelization have been developed in the Earth Simulator Center for the ocean component. Currently, we have implemented BiCGSTAB method to our ocean simulation code. In preliminary experiments, ratio of vectorization, averaged vector length and rate of parallelization were 99.65%, 250.1 and 96.0%, respectively, for core of Poisson solver with 100 km resolution for horizontal. Reduction of communication cost is present subject for optimization. Implementation of multi grid methods has completed, however, data is not shown.

5. Conclusions and near future work

Preliminary results of validation for both atmosphere and ocean components were presented. Both prototypes have been almost completed. We have just been kick off status to reproduce nonhydrostatic phenomena such as typhoon, heavy rain in Baiu season, tornado and so on. After implementing selected physical schemes, those simulations with the atmosphere component will be started from summer of 2004. Nonhydrostatic ocean code including tide scheme is also getting ready for simulation with ultra high resolution. Ultra high resolution simulation with nonhydrostatic coupled atmosphere and ocean code will be promoted not only for global but regional simulation on the Earth Simulator. Simulations with the nonhydrostatic coupled code will begin in autumn of 2004.